



Evaluation of microvasculopathy using dual-energy computed tomography in patients with chronic thromboembolic pulmonary hypertension

Onishi, Hiroyuki ; Taniguchi, Yu ; Matsuoka, Yoichiro ; Yanaka, Kenichi ; Izawa, Yu ; Tsuboi, Yasunori ; Mori, Shumpei ; Kono, Atsushi ;...

(Citation)

Pulmonary Circulation, 11(1):1-9

(Issue Date)

2021-01-01

(Resource Type)

journal article

(Version)

Version of Record

(Rights)

© The Author(s) 2021.

This article is distributed under the terms of the Creative Commons Attribution-NonCommercial 4.0 License (<https://creativecommons.org/licenses/by-nc/4.0/>) which permits non-commercial use, reproduction and distribution of the work without further...

(URL)

<https://hdl.handle.net/20.500.14094/90007860>



Evaluation of microvasculopathy using dual-energy computed tomography in patients with chronic thromboembolic pulmonary hypertension

Hiroyuki Onishi¹, Yu Taniguchi¹, Yoichiro Matsuoka¹, Kenichi Yanaka¹, Yu Izawa¹, Yasunori Tsuboi¹, Shumpei Mori¹, Atsushi Kono², Kazuhiko Nakayama^{1,3}, Noriaki Emoto^{1,4} and Ken-ichi Hirata¹

¹Division of Cardiovascular Medicine, Department of Internal Medicine, Kobe University Graduate School of Medicine, Kobe, Japan; ²Department of Radiology, Kobe University Graduate School of Medicine, Kobe, Japan; ³Department of Cardiology, Shinko Memorial Hospital, Kobe, Japan; ⁴Department of Clinical Pharmacy, Kobe Pharmaceutical University, Kobe, Japan

Abstract

The existence of microvasculopathy in patients with chronic thromboembolic pulmonary hypertension has been suggested. Recently, dual-energy computed tomography has been used to produce a sensitive iodine distribution map in lung fields to indicate microvasculopathy according to poor subpleural perfusion. Our aim was to evaluate the impact of microvasculopathy on pathophysiology in chronic thromboembolic pulmonary hypertension. According to the extent of poor subpleural perfusion, ninety-three interventional treatment-naïve patients were divided into poorly perfused ($n = 49$) or normally perfused group ($n = 44$). We assessed cardiopulmonary exercise test, right heart catheterization, and dual-energy computed tomography parameters for quantitative evaluation of lung perfusion of blood volume score. Lung perfusion of blood volume score in normally perfused group was significantly inversely correlated with pulmonary vascular resistance (pulmonary vascular resistance = $6816.1 \times$ lung perfusion of blood volume score^{-0.793}, $R^2 = 0.225$, $p < 0.01$), but lung perfusion of blood volume score in poorly perfused group was not. Poorly perfused group had higher pulmonary vascular resistance (879 ± 409 dynes-s/cm⁵ vs. 574 ± 279 dynes-s/cm⁵, $p < 0.01$) and lower lung perfusion of blood volume score (22.1 ± 5.4 vs. 26.4 ± 6.6 , $p < 0.01$) and % diffusing capacity for carbon monoxide divided by the alveolar volume ($59.9 \pm 15.4\%$ vs. $78.8 \pm 14.2\%$, $p < 0.01$). Perfusion of blood volume score in the normally perfused group showed an inverse correlation with pulmonary vascular resistance; however, that in poorly perfused group did not. Microvasculopathy might contribute to severe hemodynamics, apart from pulmonary vascular obstruction. In our experience, more than half of treatment-naïve chronic thromboembolic pulmonary hypertension patients have microvasculopathy.

Keywords

chronic thromboembolic pulmonary hypertension, dual-energy computed tomography, microvasculopathy, hemodynamics

Date received: 30 August 2020; accepted: 1 December 2020

Pulmonary Circulation 2021; 11(1) 1–9

DOI: 10.1177/2045894020983162

Introduction

Chronic thromboembolic pulmonary hypertension (CTEPH) is characterized by stenosis and obstruction of the pulmonary arteries by non-resolving, organized thromboemboli, leading to elevated pulmonary vascular resistance (PVR), severe pulmonary hypertension (PH), and right heart failure.^{1,2} Various factors are involved in the development of PH in patients with CTEPH. Recent insights have revealed that, apart from mechanical obstruction by organized thrombi in large and/or middle-sized pulmonary

arteries, peripheral microvasculopathy (small pulmonary vessel disease) is also likely to contribute to the development and progression of the disease.^{3,4} The histological changes in microvasculopathy are similar to those observed in

Corresponding author:

Yu Taniguchi, Division of Cardiovascular Medicine, Department of Internal Medicine, Kobe University Graduate School of Medicine, 7-5-2 Kusunoki-cho, Chuo-ku, 6500017, Kobe, Japan.

Email: yu.taniguchi007@gmail.com



Creative Commons Non Commercial CC BY-NC: This article is distributed under the terms of the Creative Commons Attribution-NonCommercial 4.0 License (<https://creativecommons.org/licenses/by-nc/4.0/>) which permits non-commercial use, reproduction and distribution of the work without further permission provided the original work is attributed as specified on the SAGE and Open Access pages (<https://us.sagepub.com/en-us/nam/open-access-at-sage>).

© The Author(s) 2021
Article reuse guidelines:
sagepub.com/journals-permissions
journals.sagepub.com/home/pul



idiopathic pulmonary arterial hypertension (PAH), including intimal thickening, intimal fibromuscular proliferation, and eccentric intimal fibrosis.^{5,6} In addition, microvasculopathy in CTEPH also involves diffuse very distal thrombosis.^{4,7}

Poor subpleural perfusion (PSP) in the capillary phase of pulmonary digital subtraction angiography is believed to reflect the existence of microvasculopathy, including diffuse very distal thrombosis.⁸ Tanabe et al. reported that PSP was related to worse outcomes and higher mortality in patients with CTEPH who underwent pulmonary endarterectomy. Taniguchi et al. reported that PSP was associated with worse hemodynamic responses to balloon pulmonary angioplasty (BPA) due to microvasculopathy with diffuse very distal thrombosis.⁷

Recently, dual-energy computed tomography (DE-CT) has emerged as a useful imaging modality for evaluating pulmonary artery structures and segmental lung perfusion. DE-CT can produce a sensitive iodine distribution map for lung fields by using low and high tube voltage X-rays to acquire two different datasets simultaneously.^{9,10} Lung vascular perfusion can be quantified by examining the perfusion blood volume (lung PBV) score, which is the average entire lung iodine density. Moreover, as with PSP in the capillary phase of digital subtraction angiography (DSA) of pulmonary arteries, the extent of hypoperfusion in the subpleural area reflected in color-coded lung PBV images in DE-CT might suggest the existence of microvasculopathy including a very distal thrombus.^{7–9}

The existence of microvasculopathy in patients with CTEPH has been suggested in recently published reports.^{4–6} However, the impact of microvasculopathy on the pathophysiology and qualitative methods of assessing microvasculopathy have not been well established. Our aim was to assess the association between pulmonary vascular perfusion and hemodynamic status in patients with CTEPH. We hypothesized that the extent of hypoperfusion in the subpleural area, reflected in color-coded lung PBV images, might suggest the existence of microvasculopathy including diffuse very distal thrombosis. Furthermore, we speculated that patients with microvasculopathy might have severely impaired hemodynamics as a result of pulmonary vascular obstruction.

Methods

This retrospective study complied with the guidelines of the Declaration of Helsinki and was approved by the ethics committee of our University (approval number: B190326). All enrolled study patients provided written informed consent to participate in the study.

Patients/study design

This observational study was carried out in consecutive patients who were diagnosed with CTEPH and underwent DE-CT for diagnosis at our University Hospital between

February 2014 and June 2019. All patients were diagnosed with CTEPH according to established clinical guidelines.¹¹ Right heart catheter and pulmonary angiography were performed for definitive diagnosis of CTEPH. Lung function, arterial blood gas composition, functional status using the New York Heart Association-functional class (NYHA-FC) classification, exercise capacity using the six-minute walk distance (6MWD), and the cardiopulmonary exercise test were routinely assessed at the time of diagnosis, and data were collected from hospital medical records.

The exclusion criteria were: (a) patients who refused to undergo DE-CT or patients with contraindications for enhanced contrast computed tomography due to renal dysfunction, (b) patients who were judged to be inappropriate due to severe right heart failure, and (c) patients who had previously undergone pulmonary endarterectomy or BPA.

Pulmonary angiography and DE-CT imaging protocol

DSA of the pulmonary arteries was performed at the time of CTEPH diagnosis using a 5 French pigtail catheter selectively in the right- and left-sided pulmonary arteries from an anterior–posterior and lateral view of each lung. In total, 25–30 ml of contrast media was injected at a flow rate 12–15 ml/s for each series. DSA arteriograms were taken at 3.75 frames/s.

DE-CT was performed using a third-generation dual-source CT scanner (SOMATOM Force; Siemens AG, Erlangen, Germany) operating in the dual-energy scan mode, with a tube A voltage of 150 kV yielding a reference of 208 mAs and a tube B voltage of 80 kV yielding a reference of 374 mAs. A test injection was performed to determine the scan delay. A 10 ml iodine-containing contrast medium (370 mgI/ml) diluted to 50% using saline was injected, followed by an injection of 20 ml saline. Contrast media was injected for 10 s at a rate of 22 mgI/kg/s. A region of interest (ROI) was designated in the main pulmonary artery, and the time–density curve within the ROI was recorded. The early phase DE-CT scan of the pulmonary artery was acquired four seconds after the test injection-mediated enhancement peaked from the base of the lung to the apex. DE-CT images were digitally recorded in the hospital's Picture Archiving and Communication System workstation. Composite images were created by fusing the high- and low-voltage images, and color-coded lung PBV images were reconstructed at 5-mm intervals in both the axial and coronal planes using the dual-energy application software *syngo* CT Workplace, VA44A (Siemens AG, Erlangen, Germany).

Evaluation of subpleural perfusion using DSA and DE-CT

We assessed subpleural perfusion on the DSA using the same methodology previously described by Tanabe et al. and Taniguchi et al.^{7,8} The subpleural area was defined as ≤ 1.5 cm (approximately one rib width) from the lateral pleura in the horizontal section.

We also assessed perfusion of the subpleural areas on DE-CT, in every 5 mm slice, with a similar methodology as that of the aforementioned DSA assessment. The subpleural perfusion on DE-CT was classified into three types according to the perfusion level: (1) normal perfusion, (2) segmental defect—no or poor perfusion spread evenly in a wedge shape due to proximal vessel occlusion, and (3) poor perfusion—nonperfusion or minimal perfusion (Fig. 1a–c). Patients were classified into either a poorly perfused group or a normally perfused group, as previously described. The normally perfused group had patients with normal perfusion of the subpleural space in at least one segment. The poorly perfused group had patients with subpleural spaces that were nonperfused or minimally perfused in all segments.^{7,8} The wedge-shaped segmental defect was considered to occur due to proximal vessel occlusion, and therefore, the area of a simple segmental defect was excluded for the purpose of classifying patients into the poorly perfused or the normally perfused group.

The assessment of DE-CT images was performed by two cardiologists blinded to the patients' identity and hemodynamic information, and the interobserver agreement was confirmed by a McNemar test for the first 50 patients ($p < 0.001$). In cases where subpleural perfusion assessment was difficult, a final consensus was reached after consulting an experienced cardiologist and radiologist (Y.T. and A.K.).

Statistical analysis

All statistical analyses were performed using SPSS Statistics 26.0 (IBM Corp., Armonk, NY). Continuous variables are expressed as mean \pm standard deviation or median and interquartile range according to variable distribution. Differences in the continuous variables such as patient age, 6MWD, lung PBV score, hemodynamic characteristics, exercise capacity, and lung function were compared using the independent Student's *t*-test for normally distributed variables and the Mann–Whitney *U* test for non-normally distributed variables. Categorical data on patient gender, NYHA-FC classification, and use of PAH-targeted medication were expressed as numbers and percentages and compared using the χ^2 test for independence. Agreement of PSP evaluation between DSA and DE-CT was confirmed by McNemar test. For all analyses, the level of statistical significance was set at $p < 0.05$.

Results

During the study period, a total of 95 patients were diagnosed with CTEPH. Among them, two patients were excluded: one owing to renal dysfunction ($n = 1$) and another was deemed inappropriate for the study owing to severe right heart failure ($n = 1$). Finally, 93 patients were enrolled in this study.

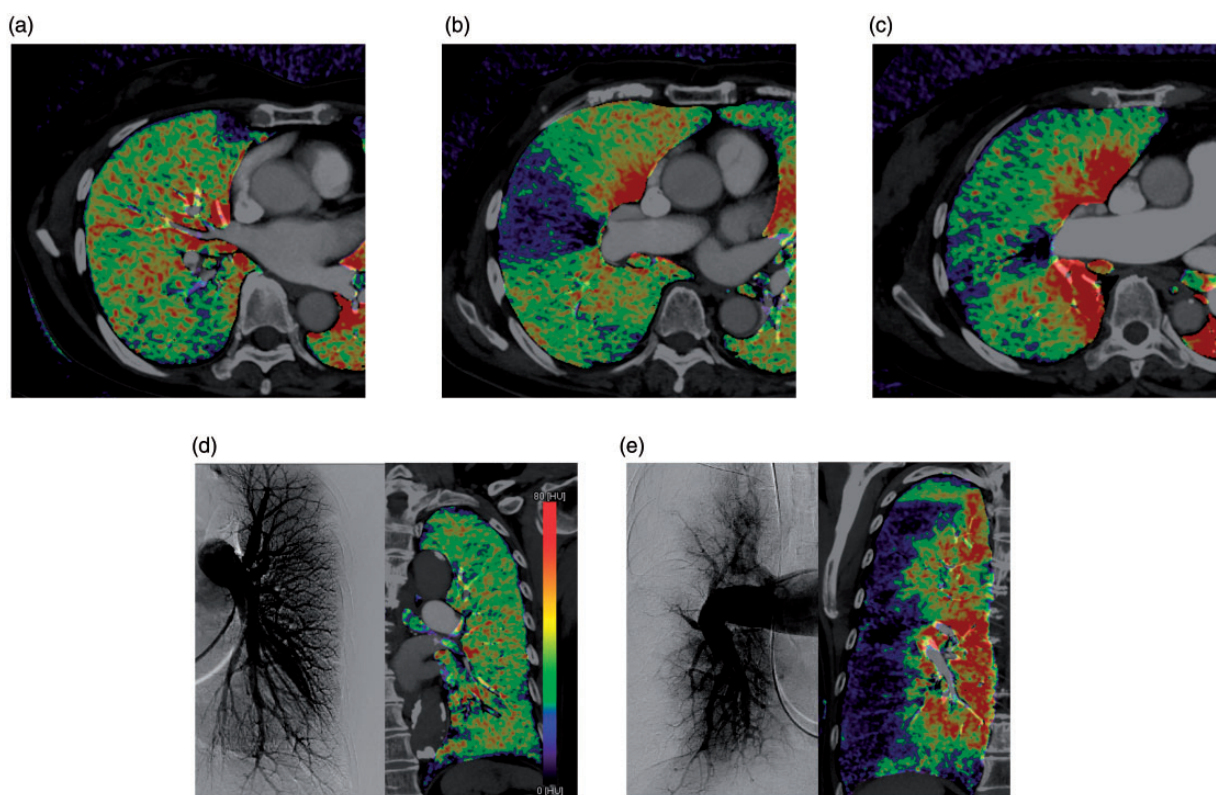


Fig. 1. Horizontal section of DE-CT in a case with: (a) normal subpleural perfusion, (b) wedge-shaped segmental defect, and (c) poor subpleural perfusion. Capillary phase of digital subtraction pulmonary angiography and DE-CT in a case with (d) normal subpleural perfusion and (e) poor subpleural perfusion.

Relationship of PSP evaluation between DSA and DE-CT

PSP in the capillary phase of DSA was observed in 38 patients (40.9%), while PSP on DE-CT was observed in 49 patients (52.7%). The concordance rate evaluated by McNemar test was $\kappa = 0.62$ (95% CI: 0.46–0.78), $p < 0.01$. PSP on DE-CT was found to well reflect the PSP on DSA of the pulmonary artery (Fig. 1d and e).

Poorly perfused group versus normally perfused group according to DE-CT

Of the 93 patients included in the analysis, 49 patients who had PSP on DE-CT were classified into the poorly perfused group and 44 patients without PSP into the normally perfused group. Patient hemodynamic data and clinical

characteristics at the time of diagnosis are summarized in Table 1. Patient characteristics including age, gender ratio, and NYHA-FC were similar between the groups. The poorly perfused group had a significantly lower lung PBV score (22.1 ± 5.4 Hounsfield unit vs. 26.4 ± 6.6 Hounsfield unit, $p < 0.01$) with worse hemodynamics, higher PVR (879 ± 409 dynes-s/cm⁵ vs. 574 ± 279 dynes-s/cm⁵, $p < 0.01$), higher mean PAP (39.7 ± 10.1 mmHg vs. 35.0 ± 10.4 mmHg, $p = 0.03$), higher systolic PAP (70.4 ± 17.0 mmHg vs. 60.1 ± 18.4 mmHg, $p < 0.01$), higher diastolic PAP (24.1 ± 7.7 mmHg vs. 20.4 ± 7.3 mmHg, $p = 0.02$), lower SvO₂ ($60.3 \pm 8.6\%$ vs. $65.7 \pm 7.7\%$, $p < 0.01$), and higher brain natriuretic peptide (BNP) level (160 (40–518) pg/ml vs. 62 (26–94) pg/ml, $p = 0.01$). In the lung function test, the poorly perfused group had a lower diffusing capacity for carbon monoxide divided by alveolar volume

Table 1. Baseline characteristics of the patient population.

Variable	Overall population (n = 93)	Poorly perfused group (n = 49)	Normally perfused group (n = 44)	p Values ^a
Baseline characteristics				
Age (years)	66.6 ± 12.8	65.8 ± 12.6	67.5 ± 13.1	0.53
Male, n (%)	21 (22.1)	14 (28.6)	7 (15.9)	0.21
NYHA-FC (I, II/III, IV) (%)	1/18/77/7	0/8/35/6	1/10/32/1	0.19
BNP (pg/ml)	80 (32–272)	160 (40–518)	62 (26–94)	<0.01
Lung PBV score (Hounsfield unit)	24.1 ± 6.3	22.1 ± 5.4	26.4 ± 6.6	<0.01
Baseline hemodynamics				
Mean RAP (mmHg)	5.2 ± 3.7	5.4 ± 4.0	5.0 ± 3.4	0.61
Systolic PAP (mmHg)	65.7 ± 18.1	70.4 ± 17.0	60.1 ± 18.4	0.01
Diastolic PAP (mmHg)	22.3 ± 7.7	24.1 ± 7.7	20.4 ± 7.3	0.02
Mean PAP (mmHg)	37.5 ± 10.4	39.7 ± 10.1	35.0 ± 10.4	0.03
PAWP (mmHg)	5.2 ± 3.7	7.8 ± 3.6	8.9 ± 4.0	0.20
Cardiac output (L/min)	3.6 ± 1.3	3.3 ± 1.2	4.0 ± 1.5	0.01
Cardiac index (L/min/m ²)	2.2 ± 0.8	2.1 ± 0.8	2.4 ± 0.7	0.05
PVR (dyne-s/cm ⁵)	734 ± 381	879 ± 409	574 ± 279	<0.01
SvO ₂ (%)	62.9 ± 8.5	60.3 ± 8.6	65.7 ± 7.7	<0.01
Exercise capacity				
6MWD (m)	323 ± 97	303 ± 101	342 ± 92	0.06
Peak VO ₂ in CPET (ml/min/kg)	12.9 ± 4.4	12.8 ± 4.3	13.1 ± 4.7	0.79
VE/VCO ₂ slope in CPET	40.5 ± 11.1	43.8 ± 10.7	37.8 ± 11.0	0.04
Lung function test				
%VC (%)	89.3 ± 17.7	88.9 ± 17.8	89.8 ± 17.9	0.82
FEV 1.0% (%)	73.3 ± 8.7	71.5 ± 9.1	75.1 ± 8.0	0.05
%DL _{CO} /VA (%)	68.8 ± 17.5	59.9 ± 15.4	78.8 ± 14.2	<0.01
Medications at baseline anticoagulation				
Warfarin, n (%)	61 (65.6)	36 (73.5)	25 (56.8)	0.13
DOAC, n (%)	32 (34.4)	13 (26.5)	19 (43.2)	0.13
PAH-specific drugs				
ERA, n (%)	8 (8.6)	5 (10.2)	3 (6.8)	0.72
PDE5-i, n (%)	4 (4.3)	2 (4.1)	2 (4.5)	1.00
sGC stimulator, n (%)	11 (11.8)	6 (12.2)	5 (11.4)	1.00

NYHA-FC: New York Heart Association-functional class; BNP: brain natriuretic peptide; PBV: perfusion blood volume; RAP: right atrial pressure; PAP: pulmonary artery pressure; PAWP: pulmonary artery wedge pressure; PVR: pulmonary vascular resistance; SvO₂: mixed venous oxygen saturation; 6MWD: six-minute walk distance; VO₂: oxygen consumption; CPET: cardio-pulmonary exercise test; VE/VCO₂: ventilatory equivalent for carbon dioxide; VC: vital capacity; FEV: forced vital capacity; DL_{CO}/VA: diffusing capacity for carbon monoxide divided by the alveolar volume; DOAC: direct oral anticoagulants; ERA: endothelin-receptor antagonists; PDE5-i: phosphodiesterase type-5 inhibitors; sGC: soluble guanylate cyclase.

Note: Data are given as mean ± standard deviation or median (interquartile range).

^aComparison between poorly perfused group and normally perfused group.

(DL_{CO}/VA) ($59.9 \pm 15.4\%$ vs. $78.8 \pm 14.2\%$, $p < 0.01$), although other parameters were similar in both groups. There was a trend of poor 6MWD exercise capacity (303 ± 101 m vs. 342 ± 92 m, $p = 0.06$) in the poorly perfused group.

All patients received oral anticoagulants (approximately 65% of patients received warfarin and 35% of patients received direct oral anticoagulants. Twenty-five percent of patients received PAH medications at the time of DE-CT; almost half of them received soluble guanylate cyclase stimulators. No relevant differences were noted between the drugs administered to patients in both the groups.

Relationship between lung PBV score and PVR

Fig. 2 shows the relationship between lung PBV score and PVR for all patients. There was a significant nonlinear and inverse correlation between them ($PVR = 7103.3 \times \text{lung PBV score}^{-0.762}$, $R^2 = 0.169$, $p < 0.01$). Patients with higher PVR generally had a lower lung PBV score in both patient cohorts. Fig. 3a and b shows the relationship between lung PBV score and PVR for patients of the poorly perfused group and normally perfused group. In the poorly perfused group, there was no significant correlation between the lung PBV score and PVR ($PVR = 2638.4 \times \text{lung PBV score}^{-0.397}$, $R^2 = 0.044$, $p = 0.15$). However, a strong nonlinear and inverse correlation was observed between the lung PBV score and PVR in the normally perfused group ($PVR = 6816.1 \times \text{lung PBV score}^{-0.793}$, $R^2 = 0.225$, $p < 0.01$).

Predictor of PSP on DE-CT in CTEPH

Results of the logistic regression analysis of variables associated with PSP on DE-CT are shown in Table 2. On univariate analysis, a lower lung PBV score and lower % DL_{CO}/VA were associated with PSP on DE-CT. Among the hemodynamic variables, a higher systolic PAP, higher PVR, and higher BNP levels were related to PSP on DE-CT. A higher VE/VCO_2 slope on the cardiopulmonary exercise test was also associated with PSP on DE-CT. On forward stepwise multivariate analysis, a high PVR (adjusted odds ratio (OR): 1.001, 95% confidence interval (CI): 1.000–1.001, $p = 0.04$) and low % DL_{CO}/VA at diagnosis were associated with PSP on DE-CT (OR: 0.912, 95% CI: 0.864–0.962, $p < 0.01$). To evaluate the optimal cut-off value of % DL_{CO}/VA , a receiver operating characteristics curve analysis was performed (Fig. 4) (area under the curve: 0.840). In this analysis, 71.2% of % DL_{CO}/VA was the optimal cut-off value predicting PSP on DE-CT in CTEPH (sensitivity: 79.2%, specificity: 76.7%).

Discussion

In this study, pulmonary perfusion of blood volume in the normally perfused group showed an inverse correlation with PVR, while that of patients in the poorly perfused group did not. Apart from pulmonary vascular obstruction, microvasculopathy may also contribute to severe hemodynamics. Although the existence of microvasculopathy was not verified by a histological examination, DE-CT might be

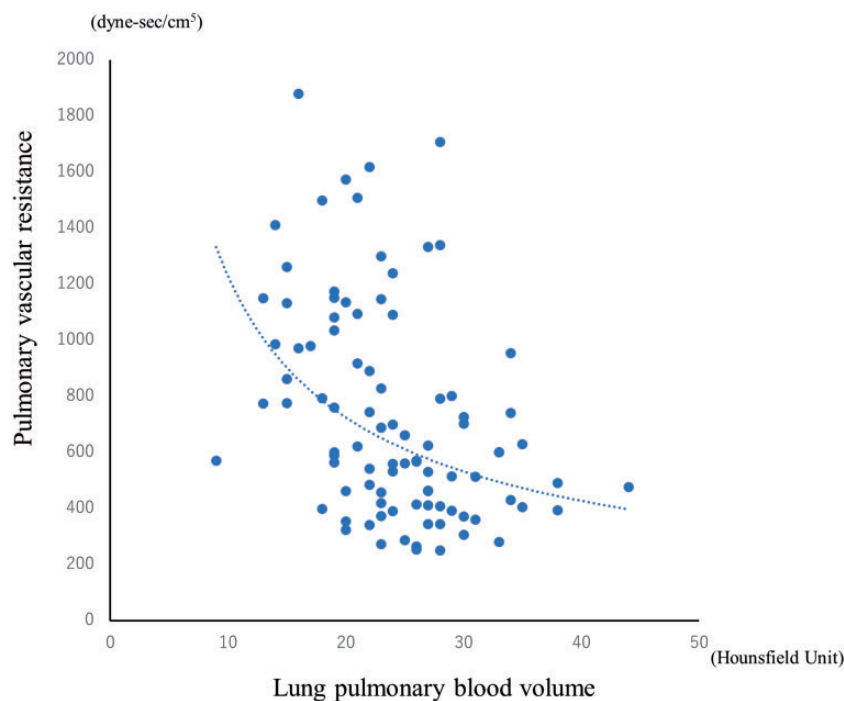


Fig. 2. The relationship between PVR obtained from right heart catheter and lung PBV score obtained from DE-CT in all patients ($n = 93$), ($PVR = 7103.3 \times \text{lung PBV score}^{-0.762}$, $R^2 = 0.169$, $p < 0.01$).

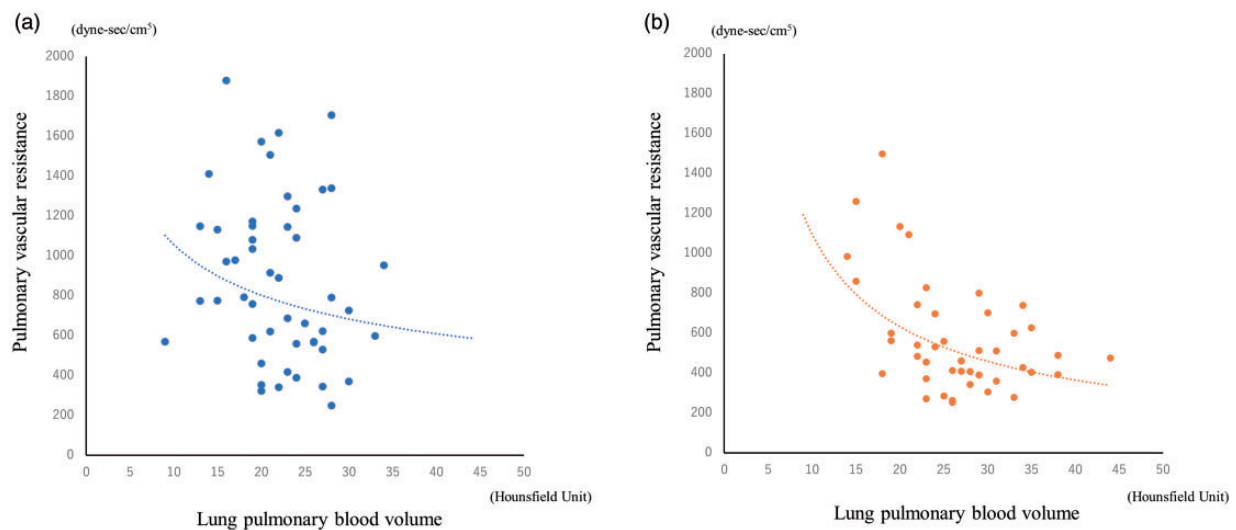


Fig. 3. The relationship between PVR obtained from right heart catheter and lung PBV score obtained from DE-CT in (a) patients of the poorly perfused group ($n = 49$) ($PVR = 2638.4 \times \text{lung PBV score}^{-0.397}$, $R^2 = 0.044$, $p = 0.15$) and (b) patients of the normally perfused ($n = 44$) ($PVR = 6816.1 \times \text{lung PBV score}^{-0.793}$, $R^2 = 0.225$, $p < 0.01$).

Table 2. Univariate and multivariate logistic regression analysis of predictive variables of microvasculopathy in CTEPH.

Variable	Univariate			Multivariate		
	OR	95% CI	p Value	OR	95% CI	p Value
Baseline characteristics						
Age (years)	0.990	0.958–1.020	0.53			
Male	2.110	0.764–5.850	0.15			
Lung PBV score (Hounsfield unit)	0.882	0.816–0.954	<0.01			
NYHA-FC (III–IV vs. I–II)	1.710	0.616–4.740	0.30			
6MWD (m)	0.996	0.991–1.000	0.06			
DL _{CO} /VA (%)	0.906	0.867–0.947	<0.01	0.912	0.864–0.962	<0.01
BNP (pg/ml)	1.001	1.000–1.001	0.01			
Peak VO ₂ in CPET (ml/min/kg)	0.984	0.877–1.100	0.79			
VE/VO ₂ slope in CPET	1.050	1.001–1.110	0.05			
Baseline hemodynamics						
Mean RAP (mmHg)	1.030	0.922–1.150	0.61			
Mean PAP (mmHg)	1.050	1.000–1.090	0.03			
Diastolic PAP (mmHg)	1.070	1.010–1.130	0.03			
PVR (dyne-s/cm ⁵)	1.002	1.001–1.002	<0.01	1.001	1.000–1.001	0.04
SvO ₂ (%)	0.921	0.872–0.974	<0.01			

OR: odds ratio; CI: confidence interval; PBV: perfusion blood volume; NYHA-FC: New York Heart Association-functional class; 6MWD: six-minute walk distance; DL_{CO}/VA: diffusing capacity for carbon monoxide divided by the alveolar volume; BNP: brain natriuretic peptide; VO₂: oxygen consumption; CPET: cardio-pulmonary exercise test; VE/VO₂: ventilatory equivalent for carbon dioxide; RAP: right atrial pressure; PAP: pulmonary artery pressure; PVR: pulmonary vascular resistance; SvO₂: mixed venous oxygen saturation.

effective in assessing microvasculopathy with PSP in CTEPH. Patients with PSP on DE-CT had a lower DL_{CO}, which might be the strongest predictor of microvasculopathy including diffuse distal thrombosis.

Microvasculopathy in CTEPH

Recent insights have revealed that peripheral microvasculopathy (small pulmonary vessel disease) has an important

role in the development and progression of CTEPH.^{3,4} The initial observations of microvasculopathy in CTEPH, reported by Moser and Bloor in 1993, revealed that “primary PH” cannot be differentiated from potentially correctable CTEPH on the basis of histopathologic findings in the small pulmonary arteries of lung tissue in patients with CTEPH, on biopsy or autopsy.¹³ Dorfmueller et al. reported that intimal fibrosis of small peripheral vessels was observed in not only small pulmonary arteries but also in pulmonary

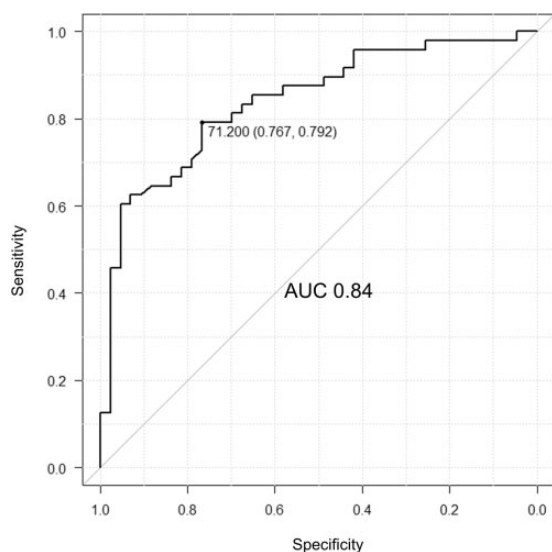


Fig. 4: The receiver operating characteristics curve of DL_{CO}/VA associated to the existence of microvasculopathy (area under the curve: 0.840).

AUC: area under the curve.

veins and capillaries from pathologic analysis of lung histology in patients with CTEPH sampled after lung transplantation or autopsy.⁵ The main mechanism inducing microvasculopathy has been thought to be endothelial shear stress and proliferation of pulmonary arterial smooth muscle in open vessels exposed to high pressure flow. However, microvasculopathy was also observed in lung regions distal to completely obstructed and partially obstructed proximal vessels. The main contributing mechanisms remain obscure.¹³ The development of hypertrophied bronchial arteries is a well-known feature in CTEPH cases.¹² They might reflect collaterals between the systemic and pulmonary arterial circulation. Mercier and Fadel reported a strong correlation between bronchial arterial hypertrophy and micro vessel remodeling in a piglet model of CTEPH, which was created by primary ligation of the left main pulmonary artery and repeated histoacryl embolization of the pulmonary artery of the right lower lobe.¹⁴ Development of microvasculopathy is secondary to exposure of the pulmonary artery circulation to high-pressure systemic circulation, owing to the development of anastomosis between bronchial arteries and the pulmonary artery.⁴ Moreover, poorly developed bronchial arteries might be involved in the development of diffuse distal thrombosis in patients with CTEPH.⁷

Evaluation of microvasculopathy in CTEPH

Although the existence of microvasculopathy including diffuse distal thrombosis in CTEPH has been proposed widely, evaluation methods for detection have not yet been established.

Kim et al. reported that a pulmonary arterial occlusion pressure waveform analysis may have been useful for the identification of significant distal, small-vessel disease in 26 patients with CTEPH. Their study demonstrated that the difference between occlusion pressure and the estimated pulmonary artery wedge pressure in the pulmonary artery occlusion technique reflected downstream resistance in small pulmonary arteries, and patients with higher downstream resistance were at high risk of mortality.¹⁵ Azarian et al. reported that a higher PAP and total pulmonary resistance were observed in patients with CTEPH ($n = 45$) than those with acute pulmonary embolism ($n = 31$), with a comparable percentage of vascular obstruction scored based on perfusion lung scans. There were no significant correlations between the percentage of vascular obstruction and PAP or total pulmonary resistance.¹⁶ Recent reports have reported that PSP in the capillary phase of digital subtraction pulmonary angiography, suggesting the presence of microvasculopathy and/or diffuse distal thrombosis, is a predictor of poor outcome of pulmonary endarterectomy for operable CTEPH and BPA for non-operable CTEPH.^{7,8} In the present study, we demonstrated the possibility of using DE-CT not only for quantifying pulmonary artery perfusion with the lung PBV score but also for qualitatively evaluating microvasculopathy, including diffuse distal thrombosis, by a more sensitive analysis of PSP in three dimensions. In this study, the lung PBV score, which represents the perfusion volume of the pulmonary artery bed, showed a strong inverse correlation with PVR in patients without microvasculopathy; however, it showed no significant correlation in patients with microvasculopathy. This might suggest that not only the degree of pulmonary vascular obstruction, but also microvasculopathy is strongly involved in the hemodynamics of CTEPH. The data might be comparable to that of an aforementioned study by Azarian et al., which demonstrated no significant correlation between the percentage of vascular obstruction and total pulmonary resistance in patients with CTEPH.¹⁶ To date, several randomized controlled trials of pulmonary vasodilators, including bosentan, riociguat, and macitentan, have reported improved PVR in patients with inoperable CTEPH. This might be because the severity of CTEPH is also characterized by microvasculopathy and could therefore be treatable by PAH-specific drugs to some extent.

Predictor of microvasculopathy in CTEPH

Suda et al. reported that a lower DL_{CO} was associated with poor outcomes in patients with CTEPH and might indicate pronounced microvasculopathy.¹⁷ Taniguchi et al. reported that a lower DL_{CO} was one of the risk factors of the failure of BPA for patients with non-operable CTEPH.⁷ It might thus be proposed that a lower DL_{CO} reflects microvasculopathy including diffuse distal thrombosis in patients with CTEPH. Our study also supports the strong correlation between lower DL_{CO} and microvasculopathy. A lower

DL_{CO}/VA was the strongest predictor of microvasculopathy including diffuse distal thrombosis, with an estimated cut-off value of 68.1% (sensitivity: 61.2%, specificity: 95.6%). However, Takei et al. reported that DL_{CO} did not show a significant improvement after BPA for non-operable CTEPH, although hemodynamics and lung function including vital capacity and forced expiratory volume 1.0% dramatically improved.¹⁸ These results meant that microvasculopathy including diffuse distal thrombosis persisted even after interventional treatment.

The incidence of microvasculopathy in CTEPH is a subject of ongoing research. Kim et al. reported that 15.3% of the 26 patients with CTEPH in one study had microvasculopathy.¹⁵ Aforementioned studies of PSP revealed that approximately 28% of patients who were operated for CTEPH and 15% of non-operable patients who underwent BPA had microvasculopathy.^{7,8} In the present study, more than half of the patients had microvasculopathy including diffuse distal thrombosis to some extent from DE-CT findings. This might be due to the different evaluation methods or definitions of microvasculopathy in CTEPH. However, Claessen et al. reported that exercise intolerance in post-pulmonary endarterectomy patients with normalized resting hemodynamics can be explained by an abnormal pulmonary vascular reserve and chronotropic incompetence.¹⁹ This suggests that more patients with CTEPH might have microvasculopathy than currently expected. Further investigations are needed to better understand the incidence of microvasculopathy.

Limitations

The main limitation of this study was its retrospective observational nature. For this reason, some missing data were unavoidable, which might have influenced the results of multivariate regression. Furthermore, this was a single-center study with a relatively small sample size owing to the invasive nature of the evaluation, raising the possibility of selection bias. Moreover, in patients with very low cardiac output or severe tricuspid regurgitation, a longer time was required for contrast media to perfuse to the subpleural area; PSP could be overestimated even though the appropriate time–density curve within the ROI was recorded. Additionally, although the range might be limited, perfusion of the subpleural areas could not be assessed in the wedge-shaped segmental defect due to complete occlusion of the proximal vessel. This might influence the analyses of PSP. Another limitation is that this study is based on the assessment of subpleural perfusion on DE-CT using the same methodology as DSA. The concordance rate evaluated by McNemar test was good; however, the existence of microvasculopathy in CTEPH was not verified by a histological examination for both imaging examinations.

Conclusion

Pulmonary perfusion of blood volume in the normally perfused group showed an inverse correlation with PVR; however, that in the poorly perfused group did not. Apart from pulmonary vascular obstruction, microvasculopathy might contribute to severe hemodynamics. DE-CT might be effective not only in quantifying pulmonary artery perfusion with the lung PBV score but also in assessing microvasculopathy with PSP in patients with CTEPH. Lower DL_{CO} might be associated with microvasculopathy including diffuse distal thrombosis. In our experience, more than half of treatment-naïve patients with CTEPH have microvasculopathy and/or small pulmonary vessel disease with diffuse distal thrombosis from DE-CT findings.

Author's contributions

All authors contributed to manuscript review and revision and approved the final version of the manuscript. Dr Yu Taniguchi, Dr Hiroyuki Onishi, and Dr Noriaki Emoto were responsible for design, analysis, and interpretation of data. Dr Yoichiro Matsuoka, Dr Hiroyuki Onishi, Dr Kenichi Yanaka, Dr Yu Izawa, Mr Yasunori Tsuboi, Dr Shumpei Mori, Dr Atsushi Kono, and Dr Kazuhiko Nakayama participated in data collection. Dr Yu Taniguchi, Dr Hiroyuki Onishi, Dr Noriaki Emoto, and Dr Ken-ichi Hirata prepared the manuscript. The Authors of this manuscript have also certified that they comply with the Principles of Ethical Publishing in Pulmonary Circulation.

Acknowledgements

We wish to acknowledge Yoko Suzuki and Mayumi Hasegawa for their help in obtaining the data for this study. We also would like to thank Editage (www.editage.com) for English language editing.

Conflict of interest

The author(s) declare that there is no conflict of interest.

Ethical approval

This study was approved by the ethics committee of Kobe University. (Kobe, Japan).

Funding

This research received no specific grant from any funding agency in the public, commercial, or not-for-profit sectors.

References

1. Hoeper MM, Mayer E, Simonneau G, et al. Chronic thromboembolic pulmonary hypertension. *Circulation* 2006; 113: 2011–2020.
2. Humbert M. Pulmonary arterial hypertension and chronic thromboembolic pulmonary hypertension: pathophysiology. *Eur Respir Rev* 2010; 19: 59–63.
3. Kim NH. Group 4 pulmonary hypertension: chronic thromboembolic pulmonary hypertension: epidemiology, pathophysiology, and treatment. *Cardiol Clin* 2016; 34: 435–441.

4. Simonneau G, Torbicki A, Dorfmüller P, et al. The pathophysiology of chronic thromboembolic pulmonary hypertension. *Eur Respir Rev* 2017; 26.
5. Dorfmüller P, Gunther S, Ghigna MR, et al. Microvascular disease in chronic thromboembolic pulmonary hypertension: a role for pulmonary veins and systemic vasculature. *Eur Respir J* 2014; 44: 1275–1288.
6. Lang IM, Dorfmüller P and Vonk Noordegraaf A. The pathobiology of chronic thromboembolic pulmonary hypertension. *Ann Am Thorac Soc* 2016; 13: S215–S221.
7. Taniguchi Y, Brenot P, Jais X, et al. Poor subpleural perfusion predicts failure after balloon pulmonary angioplasty for non-operable chronic thromboembolic pulmonary hypertension. *Chest* 2018; 154: 521–531.
8. Tanabe N, Sugiura T, Jujo T, et al. Subpleural perfusion as a predictor for a poor surgical outcome in chronic thromboembolic pulmonary hypertension. *Chest* 2012; 141: 929–934.
9. Nakazawa T, Watanabe Y, Hori Y, et al. Lung perfused blood volume images with dual-energy computed tomography for chronic thromboembolic pulmonary hypertension: correlation to scintigraphy with single-photon emission computed tomography. *J Comput Assist Tomogr* 2011; 35: 590–595.
10. Yoshizumi T. Dual energy CT in clinical practice. *Med Phys* 2011; 38: 6346.
11. Galie N, Humbert M, Vachiery JL, et al. 2015 ESC/ERS guidelines for the diagnosis and treatment of pulmonary hypertension: the Joint Task Force for the Diagnosis and Treatment of Pulmonary Hypertension of the European Society of Cardiology (ESC) and the European Respiratory Society (ERS): endorsed by: Association for European Paediatric and Congenital Cardiology (AEPC), International Society for Heart and Lung Transplantation (ISHLT). *Eur Heart J* 2016; 37: 67–119.
12. Endrys J, Hayat N and Cherian G. Comparison of broncho-pulmonary collaterals and collateral blood flow in patients with chronic thromboembolic and primary pulmonary hypertension. *Heart* 1997; 78: 171–176.
13. Moser KM and Bloor CM. Pulmonary vascular lesions occurring in patients with chronic major vessel thromboembolic pulmonary hypertension. *Chest* 1993; 103: 685–692.
14. Mercier O and Fadel E. Chronic thromboembolic pulmonary hypertension: animal models. *Eur Respir J* 2013; 41: 1200–1206.
15. Kim NH, Fesler P, Channick RN, et al. Preoperative partitioning of pulmonary vascular resistance correlates with early outcome after thromboendarterectomy for chronic thromboembolic pulmonary hypertension. *Circulation* 2004; 109: 18–22.
16. Azarian R, Wartski M, Collignon MA, et al. Lung perfusion scans and hemodynamics in acute and chronic pulmonary embolism. *J Nucl Med* 1997; 38: 980–983.
17. Suda R, Tanabe N, Ishida K, et al. Prognostic and pathophysiological marker for patients with chronic thromboembolic pulmonary hypertension: usefulness of diffusing capacity for carbon monoxide at diagnosis. *Respirology* 2017; 22: 179–186.
18. Takei M, Kataoka M, Kawakami T, et al. Respiratory function and oxygenation after balloon pulmonary angioplasty. *Int J Cardiol* 2016; 212: 190–191.
19. Claessen G, La Gerche A, Dymarkowski S, et al. Pulmonary vascular and right ventricular reserve in patients with normalized resting hemodynamics after pulmonary endarterectomy. *J Am Heart Assoc* 2015; 4: e001602.